Available online at www.sciencedirect.com
SCIENCE DIRECT®
PERGAMON
Phytochemistry 64 (2003) 773–779
PHYTOCHEMISTRY
www.elsevier.com/locate/phytochem

Anti-plasmodial activities and X-ray crystal structures of rotenoids from *Millettia usaramensis* subspecies *usaramensis*

Abiy Yenesew[a,*], Solomon Derese[a], Jacob O. Midiwo[a], Hellen A. Oketch-Rabah[b], John Lisgarten[a,c], Rex Palmer[c], Matthias Heydenreich[d], Martin G. Peter[d], Hosea Akala[e], Julia Wangui[e], Pamela Liyala[e], Norman C. Waters[e]

[a]*Department of Chemistry, University of Nairobi, PO Box 30197, Nairobi, Kenya*
[b]*Department of Pharmacology and Pharmacognosy, University of Nairobi, PO Box 30197, Nairobi, Kenya*
[c]*Department of Crystallography, Birkbeck College, University of London, Malet Street, London, WC1E 7HX, UK*
[d]*Institut für Chemie, Universität Potsdam, PO Box 60 15 53, D-14415 Potsdam, Germany*
[e]*United States Army Medical Research Unit-Kenya MRU 64109, APO, AE 09831-4109, USA*

Received 13 November 2000; received in revised form 30 May 2003

Abstract

The dichloromethane extract of the stem bark of *Millettia usaramensis* subspecies *usaramensis* showed anti-plasmodial activity against the chloroquine sensitive (D6) and chloroquine resistant (W2) strains of *Plasmodium falciparum*. Chromatographic separation of the extract led to the identification of a new rotenoid, (6a*R*,12a*S*)-2,3-methylenedioxy-9-methoxy-8-(3,3-dimethylallyl)-12a-hydroxyrotenoid (trivial name, usararotenoid C) along with known flavonoids (usararotenoid A, 12a-epimillettosin, 6a,12a-dehydromillettone, barbigerone and 4′-*O*-geranylisoliquiritigenin) as the anti-plasmodial principles. The structures were determined by spectroscopic analyses. CD and X-ray analyses established absolute configurations.

Keywords: *Millettia usaramensis* subspecies *usaramensis*; Leguminosae; Stem bark; Rotenoids; Usararotenoid A; 12-Dihydrousararotenoid A; Usararotenoid C; NMR; CD; X-ray; Anti-plasmodial; Malaria; *Plasmodium falciparum*

1. Introduction

Due to the rising prevalence of *Plasmodium falciparum* resistance to chloroquine and other anti-malarial drugs, the treatment of malaria is becoming increasingly difficult (Winstanley et al., 2002; Hyde, 2002). This has resulted in interest in the search of anti-malarial agents from plants. Activities have been observed in different classes of plant metabolites, including flavonoids. Among the flavonoids, the chalcones have attracted the most attention and are being pursued as potential drugs against malaria (Li et al., 1995; Liu et al., 2001). Information on isoflavonoids with respect to anti-malarial activities is very scanty, however, the recent report on the anti-plasmodial activities of some isoflavones from *Andira inermis* is worth noting (Kraft et al., 2000).

The genus *Millettia* (Leguminosae) is a rich source of isoflavonoids (Dewick, 1994). In Kenya this genus is represented by six species (Beentje, 1994). Phytochemical investigation of two of these, *M. dura* and *M. usaramensis* subsp. *usaramensis*, have resulted in the isolation of a number of isoflavones, rotenoids and chalcones (Yenesew et al., 1996, 1997, 1998). Here we report a new anti-plasmodial rotenoid from *M. usaramensis* subsp. *usaramensis* along with known flavonoids.

2. Results and discussion

The dichloromethane extract of the stem bark of *Millettia usaramensis* subspecies *usaramensis* showed anti-plasmodial activity against the chloroquine-sensitive (D6) and chloroquine-resistant (W2) strains of *Plasmodium falciparum* with IC_{50} values of 21.1 and 28.0 μg/ml respectively. Chromatographic separation of

* Corresponding author: Tel.: +254-20-444-9004x2170; fax: +254-20-444-6138.
E-mail address: ayenesew@uonbi.ac.ke (A. Yenesew).

0031-9422/03/$ - see front matter © 2003 Elsevier Ltd. All rights reserved.
doi:10.1016/S0031-9422(03)00373-X

the extract led to the isolation of a new rotenoid (**1**) along with known flavonoids as the anti-plasmodial principles of this plant.

The isolation and structure elucidation of the rotenoids **2**–**4** from the stem bark of *M. usaramensis* subsp. *usaramensis* has been previously reported (Yenesew et al., 1998). The stereochemical assignment at the B/C-ring junction as 6a*R*,12a*S* for these rotenoids was based on comparison of the CD curves with other rotenoids having *trans*-B/C ring junction but opposite (6a*S*,12a*R*) configurations at C-6a and C-12a (Lami et al., 1990). We have now generated X-ray crystal structures for usararotenoid A (**2**) and 12-dihydrousararotenoid A (**3**) and confirmed these stereochemical assignments.

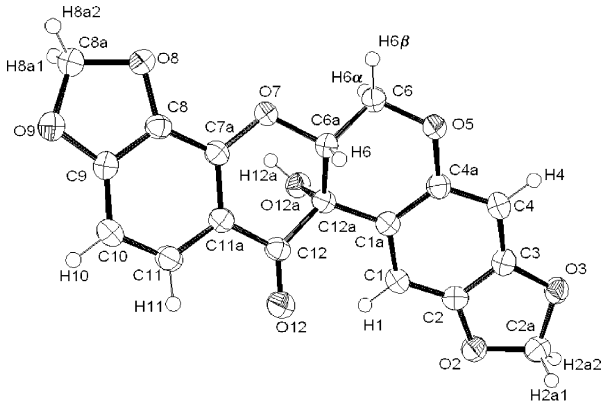

Fig. 1. ORTEP diagram showing the atom numbering scheme and solid-state conformation of **2**.

The fractional coordinates of the non-hydrogen atoms of compounds **2** and **3** are given in Tables 1 and 2 respectively. Views of the solid-state conformations are shown in Figs. 1 and 2. These molecules have normal geometry (Allen et al., 1987). The benzyl ring, D, of the 8,9-methylenedioxyphenyl moiety is planar in both compounds. The rms displacement of the six atoms from the plane is 0.018 Å in compound **2** and 0.013 Å in **3**. This plane in **2** has a dihedral angle of 5.45(0.10)° with the plane through the atoms O(8), O(9), C(8a), C(9), C(8) of ring D′; while in **3** the dihedral angle is 1.48(0.29)°. The five atoms of ring D′ in both compounds have an rms displacement of 0.097 Å from the plane, with atoms O(8) and O(9) having deviations of −0.1152 (0.0013) and −0.1078 (0.0014) Å respectively for **2** and deviations of 0.0510 (0.0027) and 0.0499 (0.0029) Å respectively for **3**. The benzyl ring, A, of the other methylenedioxyphenyl moiety is also planar in both compounds. The rms displacement of the six atoms from the plane being 0.013 Å in **2** and 0.010 Å in **3**. The plane in compound **2** has a dihedral angle of 3.57 (0.10)° with the plane of the atoms O(2), O(3), C(2), C(2a), C(3) of ring A′ while in **3** the dihedral angle is 2.16(0.34)°. The five atoms of this ring have an rms displacement of 0.064 Å in **2** and 0.033

Table 1
Atomic coordinates ($\times 10^4$) and equivalent isotropic displacement parameters ($Å^2 \times 10^3$) for **2**. *U* (eq) is defined as one third of the trace of the orthogonalized U^{ij} tensor

	x	*y*	*z*	*U*(eq)
C(1)	4936(3)	4681(2)	4924(1)	31(1)
C(1a)	6671(3)	4218(2)	5134(1)	29(1)
C(2)	4544(3)	4807(2)	4125(1)	31(1)
O(2)	2968(2)	5252(1)	3782(1)	37(1)
C(2a)	3155(3)	5034(2)	2941(2)	36(1)
C(3)	5800(3)	4517(2)	3538(1)	32(1)
O(3)	5060(2)	4736(1)	2787(1)	34(1)
C(4a)	7936(3)	3970(2)	4524(1)	30(1)
O(5)	9666(2)	3538(1)	4667(1)	34(1)
C(6)	10 336(3)	3643(2)	5474(1)	31(1)
C(6a)	8825(3)	3247(2)	6032(1)	28(1)
O(7)	9589(2)	3188(1)	6835(1)	29(1)
C(8)	8899(3)	2517(2)	8138(1)	30(1)
O(8)	10 685(2)	2357(1)	8400(1)	33(1)
C(8a)	10 479(3)	2175(2)	9252(1)	34(1)
C(9)	7652(3)	2170(2)	8715(1)	31(1)
O(9)	8607(2)	1798(2)	9375(1)	37(1)
C(10)	5765(3)	2175(2)	8590(1)	35(1)
C(11)	5156(3)	2590(2)	7869(1)	34(1)
C(11a)	6378(3)	2972(2)	7275(1)	29(1)
C(12)	5644(3)	3517(2)	6542(1)	29(1)
O(12)	3997(2)	3642(2)	6442(1)	47(1)
C(12a)	7176(3)	4019(2)	6004(1)	28(1)
O(12a)	7607(2)	5071(1)	6367(1)	32(1)

Table 2
Atomic coordinates ($\times 10^4$) and equivalent isotropic displacement parameters ($Å^2 \times 10^3$) for **3**. *U* (eq) is defined as one third of the trace of the orthogonalized U^{ij} tensor

	x	*y*	*z*	*U* (eq)
C(1a)	7105(4)	4209(5)	6444(4)	23(1)
C(1)	7234(4)	2445(4)	7006(4)	24(1)
C(2)	6538(4)	2174(4)	7874(3)	25(1)
O(2)	6532(3)	581(3)	8557(3)	39(1)
C(2a)	5535(5)	940(5)	9254(4)	30(1)
O(3)	5144(3)	2839(3)	9095(3)	33(1)
C(3)	5730(4)	3501(5)	8218(4)	25(1)
C(4)	5612(4)	5231(5)	7722(4)	28(1)
C(4a)	6323(4)	5559(4)	6837(4)	23(1)
O(5)	6124(3)	7294(3)	6342(3)	30(1)
C(6)	7037(4)	7810(5)	5613(4)	27(1)
C(6a)	7040(4)	6297(5)	4708(4)	22(1)
O(7)	7796(3)	6958(3)	3885(2)	24(1)
C(7a)	8055(4)	5626(4)	3111(4)	21(1)
C(8)	8476(4)	6192(5)	2107(4)	22(1)
O(8)	8733(3)	7958(3)	1797(3)	31(1)
C(8a)	9032(6)	7787(5)	630(5)	38(1)
O(9)	9211(3)	5895(3)	400(3)	38(1)
C(9)	8756(4)	4970(5)	1297(4)	25(1)
C(10)	8597(4)	3123(5)	1400(4)	26(1)
C(11)	8163(4)	2558(5)	2417(4)	23(1)
C(11a)	7930(4)	3765(4)	3293(3)	21(1)
C(12)	7602(5)	3064(4)	4453(4)	23(1)
O(12)	8543(3)	1567(3)	5036(3)	31(1)
C(12a)	7794(4)	4600(4)	5436(4)	22(1)
O(12a)	9337(3)	5056(3)	5978(2)	24(1)

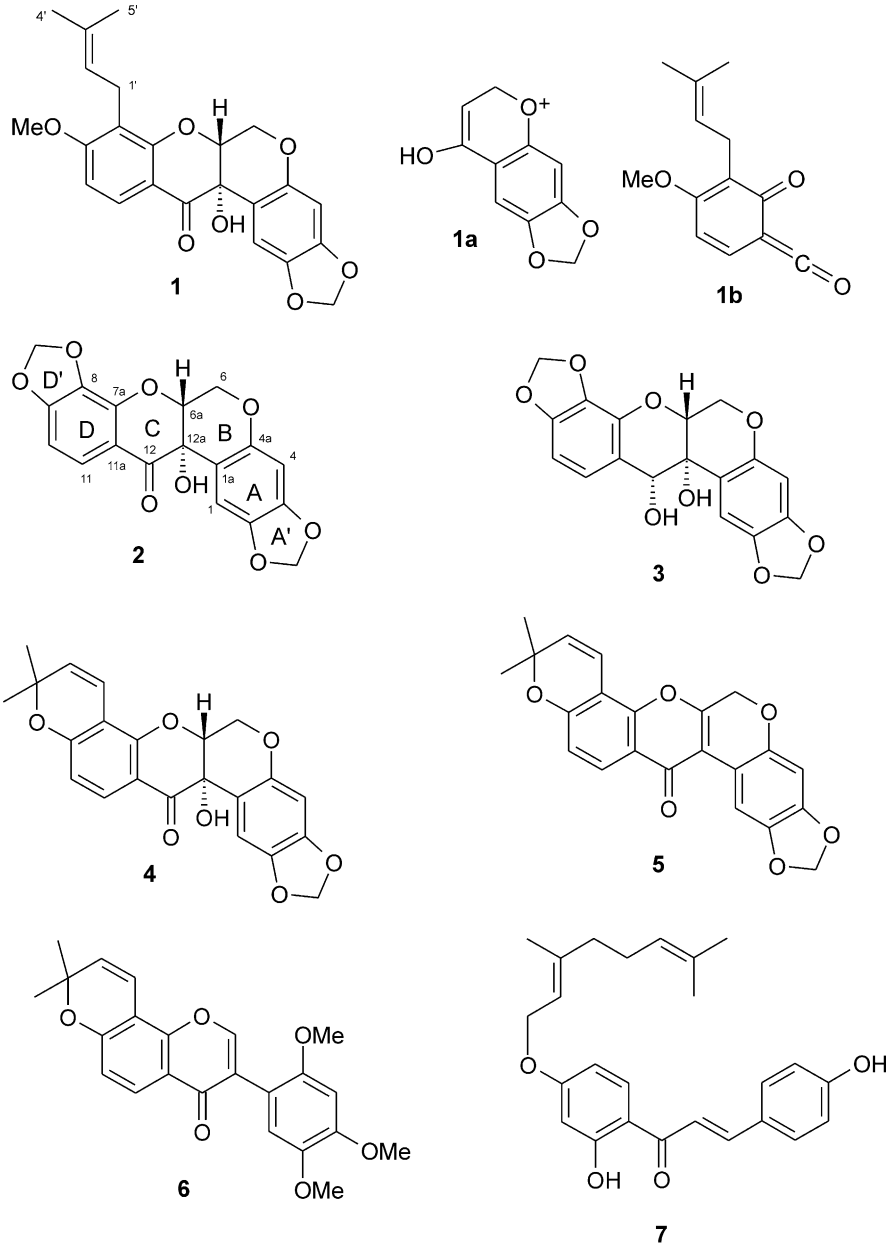

Å in **3** from the plane, with atoms O(2) and O(3) having deviations of 0.0780 (0.0013) and 0.0676 (0.0013) Å respectively in compound **2** while the deviation in **3** is 0.0414 (0.0025) and 0.0324 (0.0025) Å respectively. In compound **2** Ring C has a twist-boat conformation and ring B is in a sofa conformation. The absolute endocyclic torsion angle between the two rings is C/B (*trans*), T C/B = 64.2 + 49.5 = 103.7°. In compound **3** Ring C has an intermediate half-chair/boat conformation and ring B is in a highly distorted half-chair conformation. The absolute endocyclic torsion angle between the two rings again is C/B (*trans*), T C/B = 66.6 + 50.6 = 117.2°.

In compound **2** the structure is stabilised by an intermolecular hydrogen bond {O(12a)–H(12a)....O(3′) where atoms are related by symmetry operation [$-x+3/2$, $-y+1$, $z+1/2$]. O(12a)–H(12a) = 0.840 Å, H(12a)–O(3′) = 2.099(4) Å, O(12a)–O(3′) = 2.909(4) Å, O(12a)–H(12a)–O(3′) = 162.0°} and an intramolecular hydrogen bond {O(12a)–H(12a)—O(7). O(12a)–H(12a) = 0.840 Å, H(4)–O(7) = 2.360(3) Å, O(4)–O(7) = 2.806(3) Å, O(12a)–H(12a)–O(7) = 113.8°}. In compound **3** the structure is stabilised by two intermolecular hydrogen bonds {O(12)–H(12)....O(12a′) where atoms are related by [$-x$, $y-1/2$, $-z+1$]. O(12)–H(12) = 0.870 Å, H(12)–O(12a′) = 2.036 (3) Å, O(12)–O12a′) = 2.860(3) Å, O(12)–H(12)–O(12a′) = 157.9°} and {O(12a)–H(12a)....O(8′) where atoms are related by [$-x+2$, $y-1/2$,$-z+1$]. O(12a)–H(12a) = 0.822 Å, H(12a)–O(8′) = 2.208 (3) Å, O(12a)–O(8′) = 2.965(3) Å, O(12a)–H(12a)–O(8′) = 153.3°}.

Both compounds, (**2**) and (**3**), demonstrate a propensity for hydrogen bonding. It is possible that the relative stability of such rotenoids, having a hydroxy substituent at the C(12a) position is because of the ability of the molecules to participate in such interactions. Further it has been observed that natural rotenoids without substituents at the C(12a) position have *cis*-fused B/C ring system (Dewick, 1994). However, when a hydroxyl group is present at C(12a) both *cis* and *trans* geometry may occur. The precise reason for this is unclear but it is possible that in the non-substituted molecule the absence of steric hindrance somehow provides for energetically favourable *cis* geometry. Further investigations, using molecular dynamics simulations, are in progress to try to establish the nature of these observations.

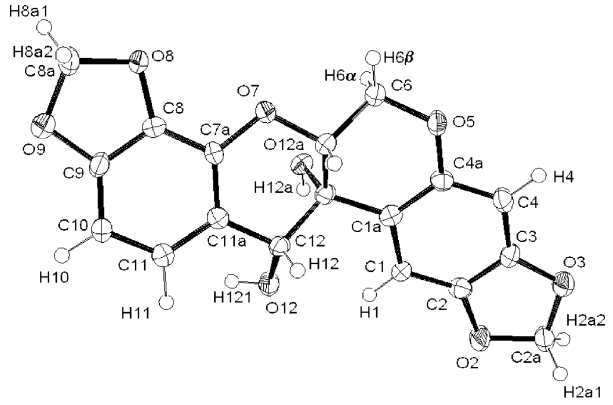

Fig. 2. ORTEP diagram showing the atom numbering scheme and solid-state conformation of **3**.

Table 3
^{1}H ($CDCl_3$ at 300 MHz) and ^{13}C ($CDCl_3$ at 75 MHz) NMR chemical shift data, together with HMBC correlations for **1**

	^{1}H	^{13}C	^2J	^3J
1	7.70 *s*	109.9	C-2	C-12a, C-3, C-4a
1a		110.5		
2		142.3		
3		149.4		
4	6.41 *s*	98.5	C-3, C-4a	C-2, C-1a
4a		150.7		
6ax	4.45 *dd*	61.7	C-6a	C-12a
6eq	4.37 *dd*		C-6a	C-12a
6a	4.60 *dd*	76.5	C-6, C-12a	
7a		158.1		
8		117.3		
9		163.3		
10	6.71 d	105.9	C-9	C-8, 11a
11	7.89 d	128.3		C-7a, C-9, C-12
11a		114.0		
12		187.6		
12a		66.5		
1′	3.37 *m*	22.1	C-8, C-2′	C-7a, C-9, C-3′
2′	5.17 *t*	121.5		Me-4′, Me-5′
3′		132.0		
4′	1.68 *s*	25.8	C-3′	C-2′, Me-5′
5′	1.77 *s*	17.8	C-3′	C-2′, Me-4′
OCH_2O	5.94 *s*	101.5		C-2, C-3
OMe	3.91 *s*	56.0		C-9
OH	2.66 *br s*			C-6a, C-1a

$J_{6ax,eq} = -9.8$ Hz, $J_{6ax,6a} = 11.8$ Hz $J_{6eq,6a} = 5.4$ *Hz*, $J_{10,11} = 8.8$ Hz, $J_{1',2''} = 7.2$ Hz.

The new rotenoid (**1**) was isolated as colourless crystals, mp 162–164 °C. The ^{1}H NMR spectrum revealed an ABX spin system at δ 4.45, 4.37 and 4.60 ($^2J_{A,B} = -9.8$, $^3J_{A,X} = 11.8$, $^3J_{B,X} = 5.4$ Hz), which is typical of the 6ax, 6eq and 6a protons of 12a-hydroxyrotenoids isolated from this plant (Yenesew et al., 1998). A methoxy, a methylenedioxy and a 3,3-dimethylallyl substituents on the 12a-hydroxyrotenoid skeleton were evident from the MS ($[M]^+$ at *m*/*z* 410), ^{1}H and ^{13}C NMR spectra (Table 3). The presence of two aromatic singlets at δ 7.70 and 6.41, in the ^{1}H NMR spectrum, and the chemical shift values of the ring A carbon atoms in the ^{13}C NMR spectrum, suggested the placement of the methylenedioxy group at C-2/C-3 position as the other rotenoids of this plant (Yenesew et al., 1998). The EIMS that showed fragment ions at *m*/*z* 191 (**1a**) as the result of RDA cleavage of ring C, is in agreement with such substitution for ring A. In the same way the fragment ion at *m*/*z* 219 (**1b**), suggested the placement of the 3,3-dimethylallyl and the methoxy groups in ring D. Two *ortho*-coupled aromatic protons at δ 6.71 and 7.89 ($J = 8.8$ Hz) were readily assigned to ring D protons, H-10 and H-11 respectively. This NMR assignment as well as biogenetic considerations allows the placement of the 3,3-dimethylallyl group at C-8 and the methoxy at C-9.

The chemical shift value for H-1 (δ 7.70) is strongly deshielded when compared to the value observed for rotenoids with *cis*-B/C ring junction (δ 6.4–6.8) indicating that the B/C ring junction in **1** has a *trans*-geometry (Oberholzer et al., 1974; Dewick, 1994). The CD spectrum (see Section 3.4) of compound **1** showed identical Cotton effects to those of usararotenoid A (**2**), usararotenoid B and 12a-epimillettosin (**4**) (Yenesew et al., 1998), and hence **1** should have the same 6a*R*,12a*S* absolute configuration. Thus this new rotenoid was identified as (6a*R*,12a*S*)-2,3-methylenedioxy-9-methoxy-8-(3,3-dimethylallyl)-12a-hydroxyrotenoid (**1**), and the trivial name usararotenoid C is suggested. The identity of this structure was confirmed from HMBC (Table 3) and HMQC experiments. 6a,12a-Dehydromillettone (**5**) (Ollis et al., 1967) was also isolated from the stem bark of this plant.

The anti-plasmodial activities of the flavonoids isolated from *M. usaramensis* subsp. *usaramensis* against *P. falciparum* are presented in Table 4. The chalcone **7** is the most potent among these flavonoids. The rotenoid **1, 4** and **5** and the isoflavone barbigerone (**6**) showed moderate activities. It is also interesting to note that compound **1** is almost three times more potent against

Table 4
In vitro IC_{50} values of flavonoids against W2 and D6 strains of *Plasmodium falciparum*

Compound	IC_{50} (μM)	
	W2	D6
1	25.8	70.1
2	66.6	60.7
3	>100	>100
4	22.2	19.4
5	33.3	39.1
6	27.0	27.3
7	8.7	10.6
Chloroquine	0.094	0.009
Quinine	0.209	0.044

the chloroquine-resistant (W2) than the chloroquine-sensitive (D6) strain, while the other compounds showed comparable activities against the two strains.

Among the rotenoids, those containing a prenyl or a 2,2-dimethylpyrano substituent are more potent than the simpler rotenoid **2**. Furthermore, no significant activity was observed for compound **3** suggesting the importance of the carbonyl function at C-12 in **2** for the weak anti-plasmodial activity observed. The isoflavone barbigerone (**6**), which has a similar substitution pattern as the rotenoids **4** and **5**, showed comparable activity with these rotenoids.

Rotenoids are known for their insecticidal properties, however, this activity is associated with those having *cis*-fused B/C ring systems; while those with *trans* B/C junction are not toxic to insects (Fukami and Nakajima, 1971). It has also been reported that rotenoids are considerably less toxic to mammals than to insects (Fukami and Nakajima, 1971). Therefore it would be of interest to test a wide range of rotenoids for anti-plasmodial activity, along with toxicity studies, in order to determine whether these rotenoids could be lead structures for clinically useful products. Such studies could also establish the structural requirement for anti-plasmodial activities.

3. Experimental

3.1. General

Analytical TLC: Merck pre-coated silica gel 60 F_{254} plates. CC on oxalic acid impregnated silica gel 60 (70–230 mesh). EIMS: direct inlet, 70 eV on a SSQ 710, Finnigan MAT spectrometer. ^{1}H NMR (300 or 200 MHz) and ^{13}C NMR (75 or 50 MHz) on Bruker or Varian-Mercury spectrometers using TMS as int. standard. HMQC and HMBC spectra were acquired using the standard Bruker software.

3.2. Plant material

Refer to Yenesew et al. (1998) for authentication of the plant material.

3.3. Extraction and isolation

Dried and ground stem bark of *M. usaramensis* subsp. *usaramensis* (1 kg) was extracted with dichloromethane and subjected to chromatographic separations as described in Yenesew et al., (1998). The 10% EtOAc in hexane eluent gave 12a-epimillettosin (Yenesew et al., 1998). The mother liquor was separated by preparative TLC (solvent system, hexane/CH_2C1_2/EtOAc; 10:5:1) to give **1** (87 mg) and **5** (7 mg). The isolation and identification of compounds **2**, **3**, **4**, **6** and **7** has already been described (Yenesew et al., 1998).

3.4. Usararotenoid C (*1*)

White crystals from CH_2Cl_2, mp 162–164 °C. $[\alpha]_D = +342°$ (MeOH, *c* 0.6). UV λ_{max} (MeOH) nm: 296. CD (MeOH, *c* 0.1). θ (λ_{max} nm): +2014 (345), −1520 (309), +1648 (280). ^{1}H NMR (Table 1). ^{13}C NMR (Table 1). EIMS *m*/*z* (rel. int.): 410 M^+ (5), 393 (9), 245 (7), 219 (67), 203 (23), 192 (83), 191 (100), 175 (20) 165 (21), 163 (25).

3.5. 6a,12a-Dehydromillettone (*5*)

Yellow crystals, mp >300 °C (lit. 355 °C). UV, IR, MS (Ollis et al., 1967). ^{1}H NMR ($CDCl_3$, 200 MHz): δ 8.33 (1H, *s*, H-1), 6.54 (1H, *s*, H-4), 4.99 (2H, *s*, H-6), 6.87 (1H, *d*, $J = 8.8$ Hz, H-10), 8.05 (1H, *d*, $J = 8.8$ Hz, H-11), 5.75 (1H, *d*, $J = 10.0$ Hz, H-3′), 6.78 (1H, *d*, $J = 10.0$ Hz, H-4′), 1.51 (6H, *s*, 2′-Me_2), 5.96 (2H, *s*, OCH_2O).

3.6. In vitro anti-plasmodial activity

The crude extract and pure compounds were assayed using an automated micro-dilution technique to determine 50% growth inhibition of cultured parasites (Chulay et al., 1983; Desjardins et al., 1979). Two different strains of *P. falciparum* parasites were cultured that are commonly used in drug sensitivity assays. The chloroquine sensitive Sierra Leone I (D6) and chloroquine resistant Indochina I (W2) strains were grown in a continuous culture supplemented with mixed gas (90% nitrogen, 5% oxygen, 5% carbon dioxide), 10% human serum, and 6% hematocrit of A+ red blood cells. Once cultures reach a parasitemia of 3% with at least a 70% ring developmental stage present, parasites were transferred to a 96 well micro titer plate with wells pre-coated with compound. The samples were serially diluted across the

plate to provide a range of concentrations used to accurately determine IC_{50} values. Plates were incubated in a mixed gas incubator for 24 h. Following the specified incubation time, ^{3}H-hypoxanthine was added and parasites allowed to grow for an additional 18 h. Cells were processed with a plate harvester (TomTec) onto filter paper and washed to eliminate unincorporated isotope. Filters were measured for activity in a micro titer plate scintillation counter (Wallac). Data from the counter was imported into a Microsoft Excel spreadsheet, which is then imported into an Oracle database/program to determine IC_{50} values.

3.7. X-ray structure analysis

Crystal data for **2.** $C_{18}H_{12}O_8$, $M_r = 356$, orthorhombic, space group $P2_12_12_1$, $a = 7.2234(2)$, $b = 12.1344(3)$, $c = 16.6245(5)$ Å, $V = 1457.16(7)$Å^{-3}, $Z = 4$, $D_c = 1.629$ g cm^{-3}, μ (MoK_α radiation, $\lambda = 0.71073$ Å) $= 0.130$ mm^{-1}, crystal size $0.4\times0.13\times0.12$ mm^3.

Crystal data for **3**. $C_{18}H_{14}O_8$, $M_r = 358$, monoclinic, space group $P2_1$, $a = 9.5522(9)$, $b = 7.3442(8)$, $c = 11.1603(15)$ Å, $\beta = 110.034(4)^\circ$, $V = 735.56(14)$ Å^{-3}, $Z = 2$, $D_c = 1.622$ g cm^{-3}, μ (MoK_α radiation, $\lambda = 0.71073$ Å) $= 0.258$ mm^{-1}, crystal size $0.2\times0.1\times0.02$ mm^3.

Preliminary unit-cell and space group information were derived in each case from oscillation and Weissenberg photographs using CuK_α radiation. Intensity data were collected using a Nonius Kappa CCD X-ray detector system provided with MoK_α radiation using liquid nitrogen as a coolant and the crystal frozen rapidly at 100 K. Data were collected by successive oscillations of the crystal. A total of 7791 and 5336 X-ray reflections were processed for **2** and **3** respectively. The data were corrected for Lorentz and polarization effects. Structure analyses were carried out using a total of 3237 and 3112 reflections with $I > 2.0\sigma(I)$ for **2** and **3** respectively.

Both structures were determined using direct methods in the SHELX program package (Sheldrick, 1986, 1993, 1997). Subsequently non-hydrogen atom types were assigned with reference to the molecular geometries. Following isotropic and then anisotropic refinement of the non-hydrogen atoms, hydrogen atoms were placed in calculated positions according to the geometry. Hydrogen atoms were subsequently included in the refinement with individual isotropic thermal displacement parameters and all refined satisfactorily. Assignment of atom types and inclusion of hydrogen atom sites have been made throughout to be consistent with the geometry of their bonding environment. No difficulties were encountered during this process. For **2**: $R = 0.043$, $wR(F^2) = 0.102$ (for observed reflections). Residual extrema in final difference map $+0.648$ to -0.251 e Å^{-3}. For **3**: $R = 0.056$, $wR(F^2) = 0.120$ (for observed reflections). Residual extrema in final difference map $+0.236$ to -0.252 e Å^{-3}.

Crystallographic calculations were performed on a Pentium PC. Geometrical calculations were performed with XANADU (Roberts and Sheldrick, 1975) and molecular illustrations were drawn with SNOOPI (Karaulov, 1994).

4. Supplementary material

Crystallographic data (excluding structure factors) for the structures reported in this paper have been deposited with the Cambridge Crystallographic Data Centre as supplementary publication. Copies of available material can be obtained, free of charge, on application to the Director, CCDC, 12 Union Road, Cambridge CB2 1EZ, UK (Fax: +44-1223-336033 or e-mail. teched@chemcrys.cam.ac.uk).

Acknowledgements

We acknowledge support by the Deutsche Forschungsgemeinschaft, Germany, Grant No. Pe 264/14-2 and by the Bundesministerium fuer Zusammenarbeit, Grant No. Pe264/14-3. Mr. S.G. Mathenge is thanked for identification of the plant material. S.D. is grateful to the German Academic Exchange Service (DAAD) and the Natural Products Research Network for Eastern and Central Africa (NAPRECA) for a scholarship.

References

Allen, F.H., Kennard, O., Watson, D.G., Brammer, L., Orpen, A.G., Taylor, R., 1987. Molecular structures and dimensions. Journal of the Chemical Society, Perkin Transactions 2, S1-S19.

Beentje, H., 1994. Kenya Trees, Shrubs and Lianas. National Museums of Kenya, Nairobi.

Dewick, P.M., 1994. Isoflavonoids. In: Harborne, J.B. (Ed.), Flavonoids: Advances in Research since 1986. Chapman and Hall, London, p. 117.

Chulay, J.D., Haynes, J.D., Diggs, C.L., 1983. *Plasmodium falciparum*: assessment of in vitro growth by [^{3}H]hypoxanthine incorporation. Experimental Parasitology 55, 138–146.

Desjardins, R.E., Canfield, C.J., Haynes, J.D., Chulay, J.D., 1979. Quantitative assessment of antimalarial activity *in vitro* by a semi-automated microdilution technique. Anti-microbial Agents and Chemotherapy 16, 710–718.

Fukami, H., Nakajima, M., 1971. Rotenone and rotenoids. In: Jacobson, M., Crosby, D.G. (Eds.), Naturally Occurring Insecticides. Marcel Dekker, New York, p. 71.

Hyde, J.E., 2002. Mechanisms of resistance of *Plasmodium falciparum* to antimalarial drugs. Microbes Infect 4, 165–174.

Karaulov, A., 1994. SNOOPI Molecular Plotting Program. School of Chemistry and Applied Chemistry, University of Wales, Cardiff.

Kraft, C., Jenett-Siems, K., Siems, K., Gupta, M.P., Bienzle, U., et al., 2000. Anti-plasmodial activity of isoflavones from *Andira inermis*. Journal of Ethnopharmacology 73, 131–135.

Lami, N., Kadota, S., Tezuka, Y., Kikuchi, T., 1990. Constituents of the roots of *Boerhaavia diffusa* L II. Structure and stereochemistry of a new rotenoid, boeravinone C. Chemical and Pharmaceutical Bulletin 38, 1558–1562.

Li, R., Kenyon, G.L., Cohen, F.E., Chen, X., Gong, B., et al., 1995. In vitro antimalarial activity of chalcones and their derivatives. Journal of Medicinal Chemistry 38, 5031–5037.

Liu, M., Wilairat, P, Go, M.L., 2001. Antimalarial alkoxylated and hydroxylated chalcones [corrected]: structure-activity relationship analysis. Journal of Medicinal Chemistry 44, 4443–4452.

Oberholzer, M.E., Rall, G.J.H., Roux, D.G., 1974. The concurrence of 12a-hydroxy- and 12a-*O*-methylrotenoids. Isolation of the first natural 12a-*O*-methylrotenoids. Tetrahedron Letters 25, 2211–2214.

Ollis, W.D., Rhodes, C.A., Sutherland, I.O., 1967. The extractives of *Millettia dura*. Tetrahedron 23, 4741–4760.

Roberts, P., Sheldrick, G.M., 1975. XANADU Program for Crystallographic Calculations. University of Cambridge, UK.

Sheldrick, G.M., 1986. SHELX86, Program for Crystal Structure Determination. University of Göttingen, Germany.

Sheldrick, G.M., 1993. SHELX93, Program for Crystal Structure Refinement. University of Göttingen, Germany.

Sheldrick, G.M., 1997. SHELX97, Program for Crystal Structure Refinement. University of Göttingen, Germany.

Yenesew, A., Midiwo, J.O., Waterman, P.G., 1996. Four isoflavones from the seed pods of *Millettia dura*. Phytochemistry 41, 951–955.

Yenesew, A., Midiwo, J.O., Waterman, P.G., 1997. 6-Methoxycalopogonium isoflavone A: a new isoflavone from the seed pods of *Millettia dura*. Journal of Natural Products 60, 806–807.

Yenesew, A., Midiwo, J.O., Waterman, P.G., 1998. Rotenoids, isoflavones and chalcones from the stem bark of *Millettia usaramensis* subspecies *usaramensis*. Phytochemistry 47, 295–300.

Winstanley, P.A., Ward, S.A., Snow, R.W., 2002. Clinical status and implications of antimalarial drug resistance. Microbes Infect 4, 157–164.